Alignment and test of a Constellation-X SXT mirror segment pair

Scott M. Owens[1], Thomas Meagher[1], Theo Hadjimichael[2], John P. Lehan[3], David A. Content[1], Timo Saha[1], William W. Zhang[1], Rob Petre[1], Paul Reid[4], William D. Jones[5], Stephen O'Dell[5]

[1]Goddard Space Flight Center (GSFC), NASA
[2]GSFC and Swales Aerospace
[3]GSFC and Universities Space Research Association
[4]Smithsonian Astrophysical Observatory
[5]Marshall Space Flight Center, NASA

ABSTRACT

A single Constellation-X Spectroscopy X-ray Telescope (SXT) mirror segment pair is being aligned in the Optical Alignment Pathfinder 2 (OAP2) platform using a combination of mechanical and optical techniques. Coarse positioning was provided through a contact probe, the alignment was refined in a collimated while-light facility used for the Suzaku (ASTRO-E2) satellite, and then finalized with a combination of a Centroid Detector Assembly (CDA) and an interferometer coupled to a novel conical null lens providing surface map imaging over 60% of the mirror surface at one time. Due to a variety of reasons, the positioning and figure of the mirror segment under examination can shift, and we test how reliably high quality alignment can be reproduced on any given day. Also, the mirror segment's deformation response to deliberate misalignments has been tested, providing a response matrix for these thin glass mirror segments.

Keywords: x-ray optics, x-ray telescope, optical alignment

INTRODUCTION

The Constellation-X Spectroscopy X-ray Telescope (SXT) is a large, segmented, modified Wolter-1 style mirror assembly, using thin slumped glass mirror segments as the reflecting elements. A significant obstacle facing the build-up of the flight mirror assembly is the mounting and alignment process to be used for the thousands of mirror segments needed. We have been investigating the fundamental mounting and alignment issues through a series of test hardware platforms known as the Optical Alignment Pathfinders (OAP). These mounting and alignment housings hold and adjust the 200 mm tall, 50 degree wide mirror segments at 5 points along each of the top and bottom edges. The first version, the OAP1, used manual micrometers for alignment, while the second generation housing, the OAP2, uses bidirectional piezoelectric bending actuators to adjust the position of the mirror segments. We are currently halfway through the alignment process of a flight-sized SXT mirror segment pair. The secondary mirror segment has been aligned, and ready to be permanently bonded into the housing. Our studies show that high quality, repeatable alignment can be done with the 10-point-style mount. Furthermore, neither gravity induced deformations nor small actuator deviations from the aligned state significantly alter the axial figure of mirror segments. We present our alignment process, the current expected imaging performance of a mirror segment pair, and the results of our mirror deformation studies when we deliberately misaligned individual actuators.

OPTICAL ALIGNMENT PATHFINDER 2

Since our last update on the Constellation-X SXT OAP2 platform,[1] a number of changes have been implemented to improve the hardware. The OAP1 precision alignment frame has been replaced with a strut frame that bolts directly to the top and bottom of the OAP2 housings, a schematic of which is shown in Figure 1. Each strut frame has a series of radial flexures with integrated piezoelectric actuators that can adjust mirror segments at 5 points along each of the top and bottom edges. The 5 mounting points are equally spaced at 12 degree intervals along the 50 degree azimuth. The flexures can be adjusted radially with a pair of set screws with a pitch of 0.2 mm/turn, and the flexures have a range of ±0.4 mm. Once aligned the flexures are locked down by tightening the opposing set screws. For more precise alignment, the bidirectional bending piezoelectric actuators are used, which have a range of approximately ±70 micrometers and provide sufficient force to adjust the local positions of mirror segments through that range. The new strut frames also provide the bonding points to hold the mirror segments in place once they have been aligned. A close up of one of the flexures in Figure 1 shows the placement of the flexure set screws, the piezo actuator, and bonding grooves.

Space Telescopes and Instrumentation II: Ultraviolet to Gamma Ray, edited by
Martin J. L. Turner, Günther Hasinger, Proc. of SPIE Vol. 6266, 62661W, (2006)
0277-786X/06/$15 · doi: 10.1117/12.672663

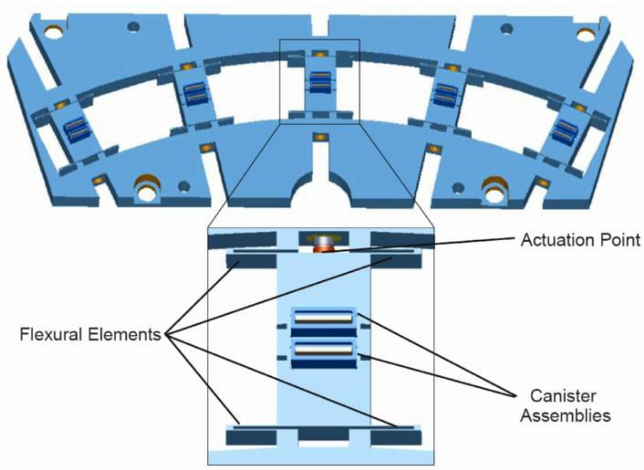

Figure 1. The new alignment strut frames used with the OAP2 housings. The design is capable of aligning and bonding two pairs of segments in the OAP2 housings.

Aside from the flexures and piezo actuators, the front faces of the OAP2 housings have been modified. Originally a 150 mm tall x 30 degree wide metrology window was cut in each front face to provide access for normal incidence axial interferometry to gauge the axial sag of mirror segments during alignment. It was recently determined that this opening did not provide sufficient access, and that a reliable prediction of the mirror segment alignment and x-ray imaging performance could not be done with only 1/2 of the mirror surface visible. As a result, most of the front surface of each OAP2 housing has been cut away, providing access for normal incidence interferometry over >90% of the mirror segment.

ALIGNMENT TOOLS AND FACILITIES

Four primary tools are used to align mirror segments. Initial placement is done with a contact coordinate measuring machine. The circularity and relative radial position of each mirror segment is then refined by monitoring the focal and intrafocal images produced when a collimated beam of white light is shone down the optical path of the mirror segments. Alignment is finalized using a combination of the Centroid Detector Assembly and an interferometer with a new refractive conical null lens set, which produces a conical wavefront that closely matches our desired mirror segment figure. Each of these tools is described in more detail below.

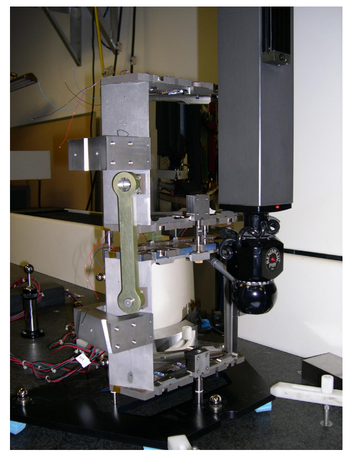

Figure 2. The contact coordinate measuring machine used to initially place mirror segments in their respective OAP2 housings.

1. Contact Coordinate Measuring Machine

Preliminary placement of the mirror segments is done by measuring the mirror segment's radial position near each of the 10 points used to adjust the segment. The position of each mounting point is adjusted using the OAP2 flexure set screws, until the position at each of the 10 mounting points is at the designed radius, within the resolution of the probe. A Renishaw PH9 probe was used, which requires a contact force of 8 g. Since the probe is a contact measurement, and our mirror segments are relatively thin, there is some deflection of the mirror segment from its static position every time a measurement is done. Modeling the deflection based on assumed mirror segment and mounting hardware stiffness yields an expected deflection during placement of up to 8 microns.

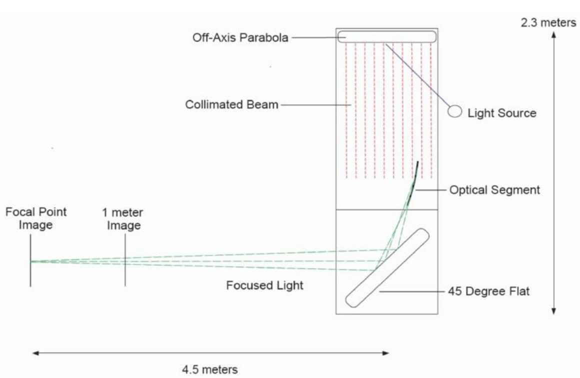

Figure 3. A schematic of the ASTRO-E vertical collimated beam alignment facility.

2.ASTRO-E collimated beam alignment facility

After initial placement of mirror segments using the contact CMM probe above, the mirror segment circularity and axial figure is refined in vertical collimated beam facility used to align the ASTRO-E x-ray telescopes. A collimated beam of while light is shone down the optical direction of the mirror segments, which is reflected and focused, within the diffraction limit of visible light. By observing that focused light at focal and intrafocal positions, we can improve the axial figure, circularity and relative radial positions of the primary and secondary mirror segments by adjusting the flexures that hold the piezo actuators.

Initial tests clearly show that the preliminary placement provided by the CMM is inadequate to align the mirror segment (s) well enough to be in the capture range of the CDA and interferometer, described below. So, an intermediate step was deemed necessary, and the collimated beam measurement provides a valuable diagnostic by providing a direct visible light focus that can be viewed at nearly any point along the optical path.

3. Centroid Detector Assembly and interferometer with conical null lens set

The Centroid Detector Assembly (CDA) is a modified Hartmann system used to gauge misalignments of grazing incidence optics. It was originally designed and used for the alignment of the HRMA on board the Chandra X-ray Observatory (AXAF).[2] It has been used in the Constellation-X SXT program for a number of years, and its application has been previously documented.[1,3] A virtual laser light source defines the position of the focus of the telescope under alignment, and the test mirror surfaces are aligned to point at that focus. By scanning the laser through a large number of azimuthal positions, the average cone angle at each point can be measured precisely.

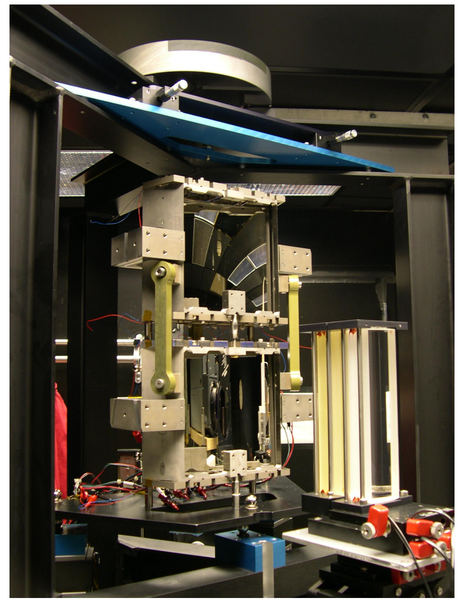

Figure 4. The OAP2-P+S stack in the CDA metrology tower. A new conical null lens set sits near the radius of curvature of the secondary mirror segment.

The CDA is a very high resolution instrument, but only provides one piece of the puzzle for alignment. The proper axial curvature must also be achieved. We measure the figure of mirror segments using a Zygo Verifire interferometer and a novel refractive conical null lens set designed in-house, shown in Figure 4. The lens set takes the central 200 mm x 50 mm section of the 200 mm diameter collimated beam to produce a conical beam with a shallow cone angle. The cone angle can be adjusted by tilting the lens set in the collimated interferometer beam. The lens set is 225 mm tall (large enough to span the 200 mm tall OAP2 mirror segments), and produces a beam that is approximately 38 degrees wide when the lens set is fully illuminated. Due to small aberrations at the edges of the wavefront we usually use only the central 30 degrees of the beam for quantitative analysis. The combination of the interferometer and null lens set allows us to image the surface figure of mirror segments with a resolution of tens of nanometers in surface height. Mapping of the conical beam onto the interferometer CCD yields a spatial resolution of 0.34 mm/pixel in the axial direction and 0.96 degrees/pixel (1.17 mm/pixel) in the azimuthal direction.

MIRROR SEGMENT ALIGNMENT AND PERFORMANCE PREDICTION

As noted above, the alignment process for a mirror segment is done in three steps. The contact CMM is used to initially place each mirror segment at approximately the correct radius, the collimated beam facility is used to refine the circularity and relative radial placement of the primary and secondary mirror segments, and the CDA and interferometer with null lens are used to perform precision alignment. The details of each step are described below.

1.Mirror segment alignment process

Initial placement of mirror segments in the OAP2 housings is done with the CMM. The contact probe measures the radial position of each mirror segment's reflecting surface as close to the actuation position as possible. The radial set screws that move each flexure are adjusted until the mirror segment surface is placed at the designed radius, within the resolution of the instrument. All measurements are done with the primary mirror segment housing (OAP2-P) stacked on top of the secondary mirror segment housing (OAP2-S). This ensures that any deformation in the secondary housing due to the added weight of the primary housing is taken into account during alignment.

After initial placement, the OAP2-P+S stack is taken to the vertical collimated beam facility most recently used to align the x-ray telescope mirrors for the Suzaku (ASTRO-E) observatory. By monitoring the intrafocal image of light reflected off of either the secondary only or the primary plus secondary combination, we can diagnose local slope angle errors as well as circularity and mounting stress, within the diffraction limit of visible light. Again, the set screws that position each radial flexure are adjusted to optimize the intrafocal image 1 meter closer to the mirror segment than the focus. (This is done with the piezo actuators powered on, and in their central position.) Once an optimum image is achieved, each pair of opposing set screws are tightened to a snug fit and Loctite is applied to the set screw threads, fixing the flexure position. A series of intrafocal images, shown in Figure 5 was taken during alignment showing the progression of alignment quality during this step. The ideal image in this case is a 50 degree arc, with no obvious light scattering or blurring at the edges of each sector of the mirror segment. The dark line through the center of the arc is an expected diffraction minimum in this orientation.

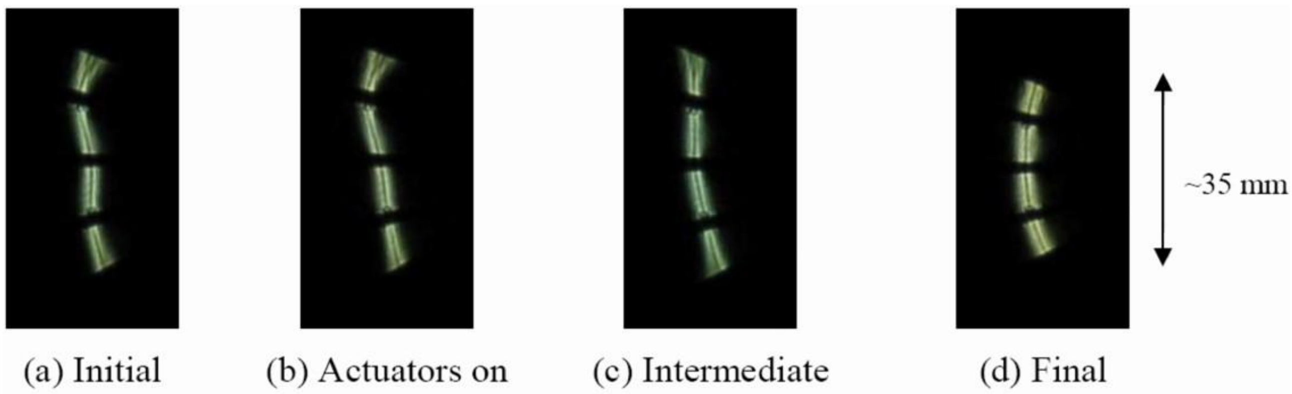

Figure 5. Intrafocal images of the secondary mirror segment in the ASTRO-E vertical collimated beam facility. By adjusting each flexure, the radial position of each mounting point is improved over the initial CMM placement.

After the collimated beam optimization is done, the OAP2 stack is moved to the CDA facility for final alignment. There the focus, as determined by the CDA, and the mirror figure, as seen by the interferometer and conical null lens, can be aligned. A typical CDA image and interferogram are shown in Figure 6. Each point in the CDA image comes from a 1 mm wide axial stripe along the mirror segment axis, and corresponds to a point along the mirror segment azimuth starting from the left hand side (the counterclockwise side, when viewed from above). Points within each group of 9 (1-9, 10-18, 19-27, 28-36) are separated by 1 degree in azimuth, with a gap of 4 degrees between each group. Points 1-9 measure the azimuthal positions at approximately 2-10 degrees from the left edge. Points 10-18 correspond to the 15-23 degree range. Points 19-27 correspond to the 27-35 degree range, and points 28-36 correspond to the 40-48 degree range. Interferometer images have a number of artifacts associated with them, the most glaring being that each image is inverted vertically. In contrast to the mirror segment orientation in Figure 4 (large diameter end pointing up), the interferometer software outputs raw data with the large diameter end at 0 mm and the small diameter end at +200 mm. Therefore, the top of the mirror segment is plotted at the bottom of each interferogram. The second, more obvious artifact is due to a 50 mm x 12 degree blockage at the bottom, azimuthal center of each housing. (Due to the inversion, this blockage shows up in the top center of each interferometer image.) As can be seen in Figure 4 that part of the interferometry window was

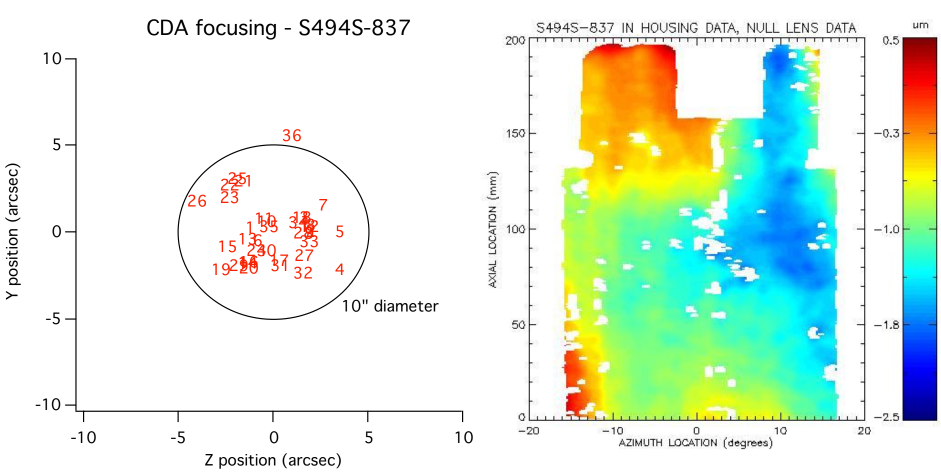

Figure 6. Typical CDA focus and mirror segment figure map.

left intact in order to mount a 2” optical reference mirror after alignment is done. The third artifact is from the mounting structure of one of the fold flats in the optical path that blocks the return beam between the 130-140 mm region, about 3.5 degree in from either side of the image. (This blockage occurs outside of the central 30 degree region, where the null lens set is most well behaved, so it does not impact the performance predictions calculated below.) Finally, there are a variety of data dropouts within each image, due to a combination of errors in the mirror segment shape, dust on the mirror segment surface, vibration in the laboratory and the inability of the interferometer software to handle high fringe density regions.

2. Secondary mirror segment alignment quality and performance prediction

Once a mirror segment is aligned (best simultaneous CDA focus and flat interferogram) a performance prediction is done to determine the expected imaging quality of the mirror segment pair. A three dimensional model of the mirror segment figure is generated from experimental data and a ray trace is performed in OSAC to produce a predicted image. The OSAC model has two primary components, derived from two different sets of data. The lower order figure (50 mm to 200 mm periods, or 0.005 mm^{-1} to 0.02 mm^{-1}) is generated by fitting the central 30 degrees of the interferogram to a Legendre/Fourier (L/F) series with 5 Legendre and 49 Fourier terms. (To account for dropouts in the raw data the IDL TRIGRID routine is used to interpolate the mirror segment figure where data does not exist.) Example raw data and a low order L/F fit are shown in Figure 7a and b. But, since there are so many dropouts in the data taken with the null lens, a second set of data must be used to determine the higher order figure (1 mm to 50 mm periods, or 0.02 mm^{-1} to 1 mm^{-1}). Before a mirror segment is chosen for use in the full alignment process, the primary metrology that is done is a set of individual axial line scans taken using a collimated beam interferometer while the mirror segment is in a 3-point vertical mount. Typically 27 lines scans are recorded, equally spaced across 50 degree wide mirror segments. It has been found that the 3-point mount does not provide repeatable low order figure, but the higher order data are reliable. The power spectral densities (PSDs) for these 27 measurements are combined into an average PSD, which is used to calculate x-ray scattering for 10 Å photons that is not taken into account in the ray trace. Individual and average PSDs for the secondary mirror segment in question are shown in Figure 7c and d.

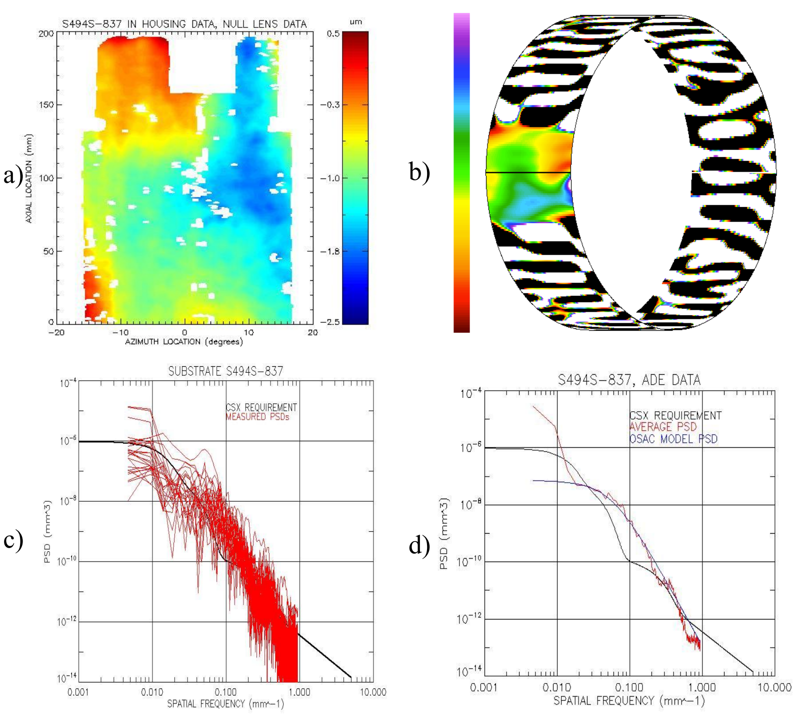

Figure 7. a) Raw interferogram. b) Legendre/Fourier fit of the raw data to a full shell surface. c) PSDs for each of 27 axial scans with the mirror segment in a 3-point mount. d) Average PSD for the entire mirror segment (red trace) and the OSAC model PSD (blue trace) used to calculate x-ray scattering. Low frequency figure errors (frequencies below 0.02 mm^{-1}) do not contribute significantly to scattering, but their effects are included in the original ray trace.

Assuming a perfect primary mirror segment, and using the low order data in Figure 7 for the secondary mirror segment, the simple ray trace yields an image quality of 6.7 arcseconds HPD, 2-reflection equivalent. Adding the x-ray scattering contribution from the higher order PSD expands that image to 9.9 arcseconds, HPD. Finally, if we assume that the low order figure of the primary mirror segment will look similar to what we measure for the secondary, then we can apply the secondary’s low order figure error to the ideal primary to obtain a realistic 2-reflection estimate. Adding the known higher order average PSD of the primary mirror segment to the calculation yields a 16.0 arcsecond HPD image.

Since the initial interferogram in Figure 7 was obtained we have improved the alignment quality and low order figure of the secondary mirror segment. We also moved the null lens set to image the left half of the mirror segment instead of the central section. (If we assume the mirror segments are essentially symmetric about their azimuthal center, the right and left halves should behave similarly.) The left hand part of Figure 8 shows interferometry data from the left half of the OAP2-S mirror segment. The data is trimmed down to the central 26 degrees, with the left half of the trimmed area aligned near to the left edge of the mirror segment. (Due to geometric constraints, only the bottom 170 mm of the mirror segment are imaged when viewing this side.) The center image shows the same data, with missing data filled in using the IDL TRIGRID function. The right hand image shows the same data, but with the axial tilt (1st order figure) removed from each column. This last image shows how uniform the sag (2nd order figure) is over the entire left half of the mirror segment. A performance prediction using this data for the low order figure of the primary and secondary mirror segments and the same higher order PSD models in Figure 7 yields an imaging quality of 13.2 arcseconds HPD for the 2-reflection system.

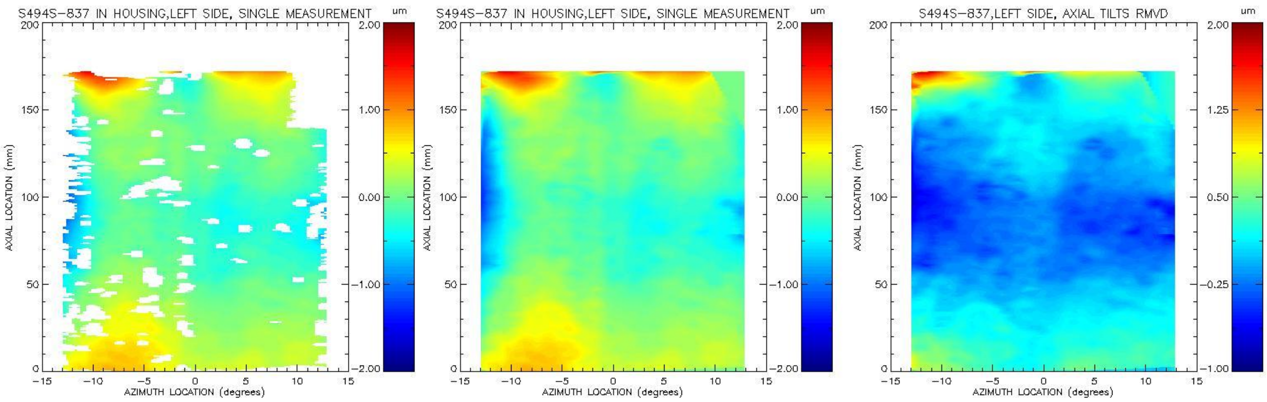

Figure 8. (left) Interferogram of the left half of the OAP2-S mirror segment. (center) Interferometry data with data dropouts filled in using the IDL TRIGRID function. (right) Same data with the axial tilt removed in each column.

3. Re-alignment repeatability

Due to a variety of environmental factors (temperature variations, vibrations, piezo actuator creep, etc.) the precise alignment of a mirror segment is subject to change slightly over time, and the alignment needs to be tuned if the system is allowed to sit and drift overnight. As such, a single alignment and performance prediction, as above, is not necessarily the best gauge of alignment quality. A more appropriate measure of how well a mirror segment pair can be aligned is a series of re-alignments over a few days or a week. On three separate days over a one week period, the OAP2-S mirror segment was realigned with interferometry and CDA data taken to gauge the alignment quality. The day to day alignment quality of these three data sets represents reliability of alignment in this system.

Figure 9 shows pairs of interferograms and CDA foci for each day. Interferometry data has dropouts filled in as before. There is clearly some change in the figure at the upper left mount point, but flattening that area out does not appear to significantly effect the global figure or the axial sag at that azimuth. The CDA foci show quite different behavior from one day to the next, but this does not appear to be reflected in the figure maps where a 1 micron change in axial tilt should correspond to a 1 arcsecond shift in focal position. Future work should include correlating the axial tilt angles inferred from by the CDA with the relative axial tilts measured by the interferometer.

Figure 10 re-plots the data from Figure 9, but with the 0th and 1st order terms removed. These images show that despite the changes in actuator positions, the global 2nd order figure (axial sag) of the mirror segment does not change much, and higher order features are clearly not effected. Furthermore, the magnitude of the axial sag is near the requirement of 1.1 micrometer P-V all the way across the images.

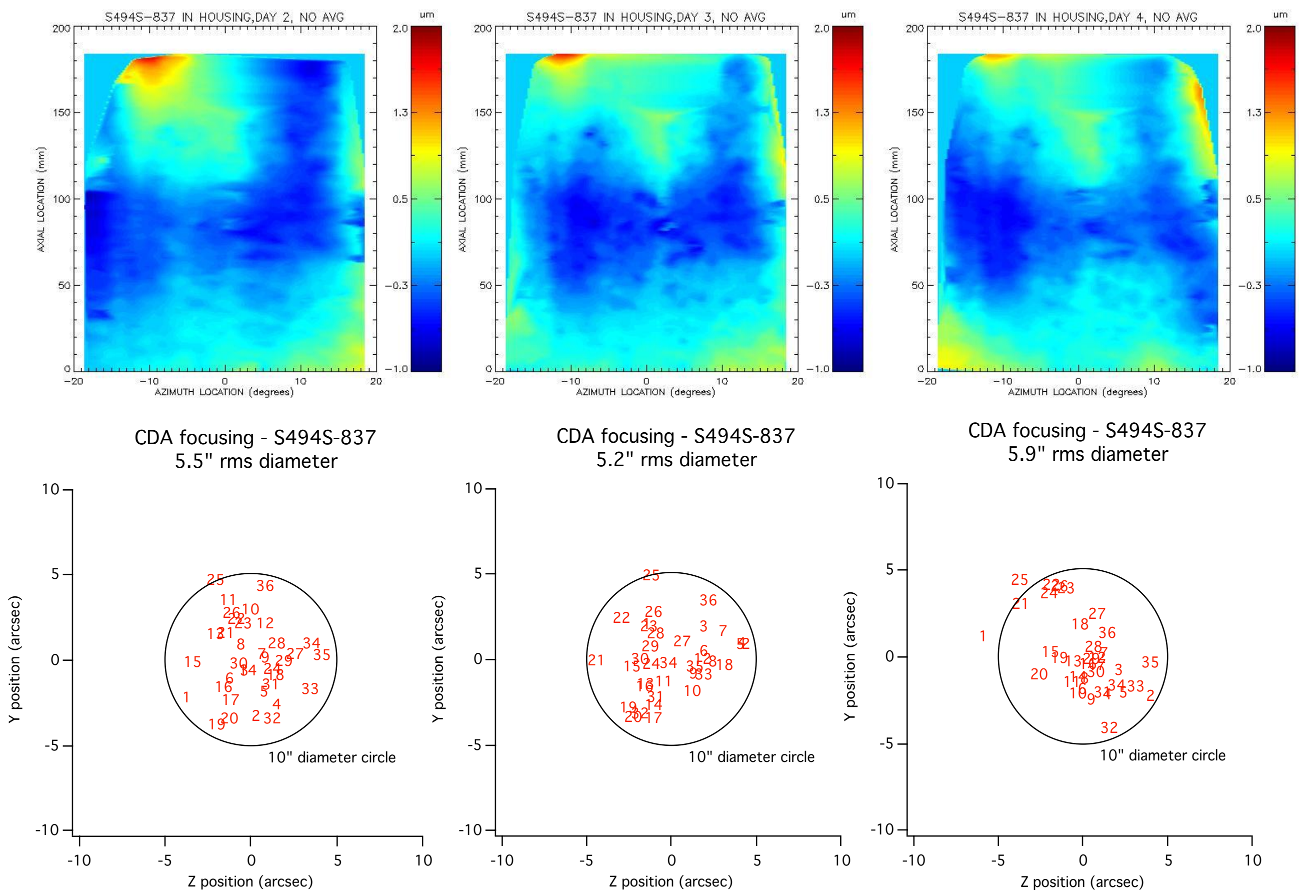

Figure 9. Interferograms and CDA foci after alignment on three sequential days.

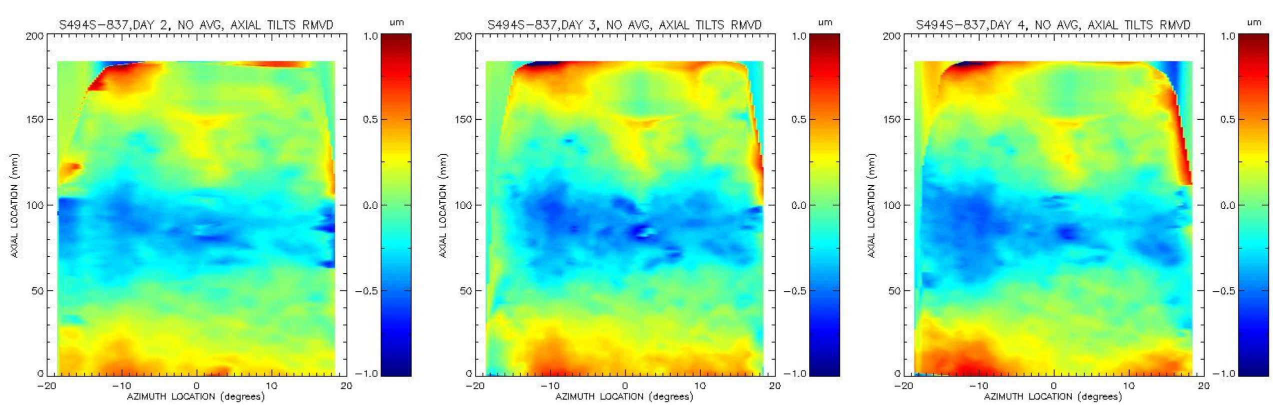

Figure 10. The same data from Figure 9 with the piston and tilt (0th and 1st order) terms removed for each column.

MIRROR SEGMENT MISALIGNMENTS – FIGURE AND IMAGE RESPONSE

In order to gauge the impact of a misalignments on mirror segment figure, we performed a series of deliberate misalignments by scanning individual actuators through a range of positions, while monitoring the mirror segment figure and CDA focus. The results show how far mounting deformations propagate through a mirror segment and the effect of alignment adjustments on local and global axial figure. Results are shown here for adjustments of the 2nd actuator from the left on the upper edge of the mirror segment, defined as actuator U2. (Again, due to the interferometer inverting data, the actuation point in these images is at 0 mm, -12 degrees.)

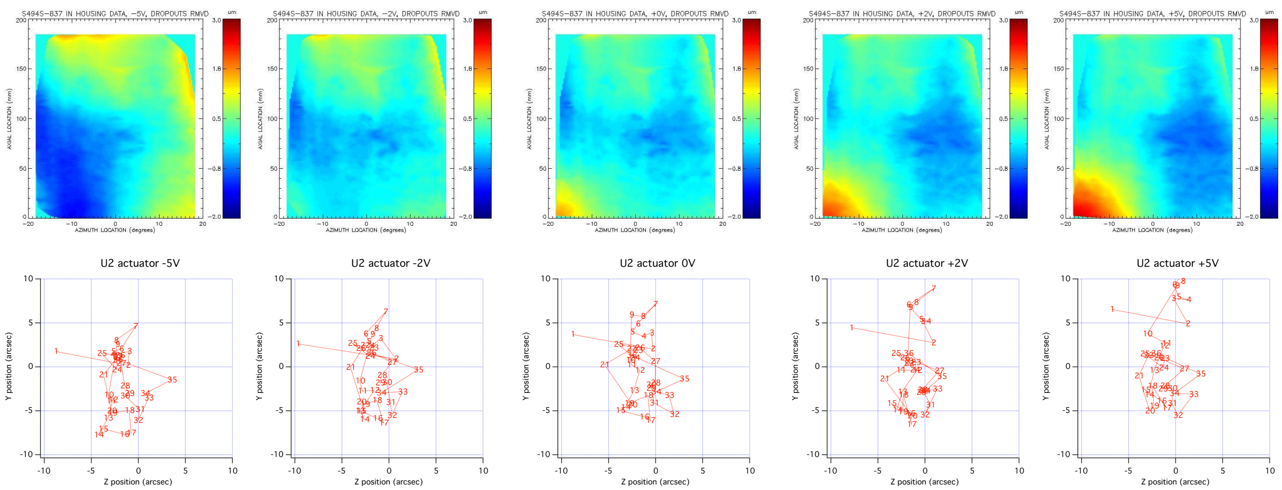

Figure 11. Secondary mirror segment figure and CDA focus at 5 different voltages for actuator U2 (0V, +/-2V, and +/-5V). The U2 actuator is located between the #9 and #10 CDA aperture positions.

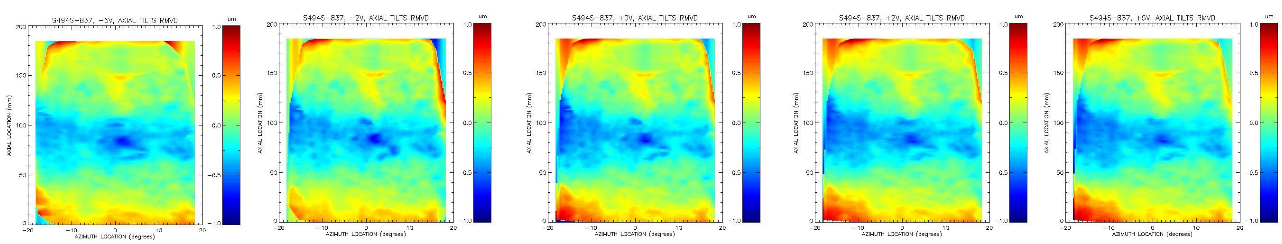

Figure 12. The same data from Figure 11, but with 0th and 1st order terms removed in each column

Figure 11 above shows figure maps for the nominal voltage ("+0V"), +/-2V, and +/-5V from the nominal. No changes to the interferometer, null lens or CDA were made during these tests. The deformation at the actuation point, as well as the effect on CDA focus can be seen in the series. From the CDA plots, it is apparent that the local tilt angle is not changed beyond the U3 actuation point (between CDA points 18 and 19).

Figure 12 shows the same figure data with 0th and 1st order terms removed. Again, it is clear how little the axial curvature or higher order shape changes, even locally. This is shown even more clearly in Figure 13 where axial profiles are plotted for azimuthal positions at -13 and +12 degrees (near to and far away from the actuation point, respectively). For each, the raw profiles, and profiles with 0th and 1st order terms removed are shown. These latter plots illustrate that the axial figure both locally and globally do not change under moderate mirror deformation.

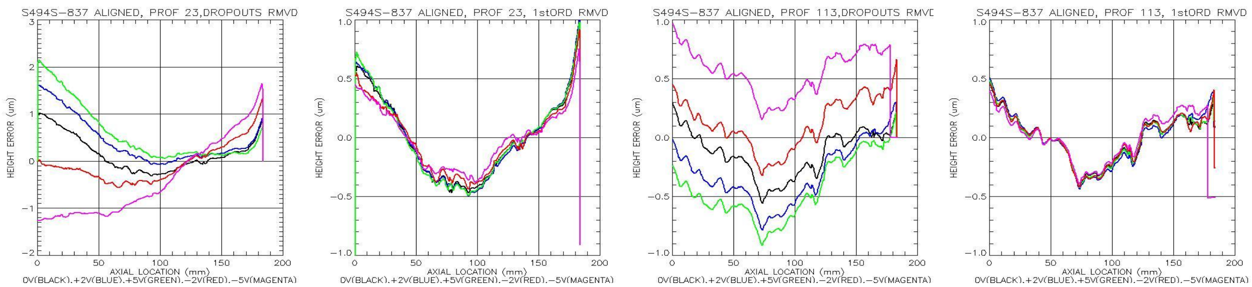

Figure 13. Axial profile data from Figure 11. The far left plot shows raw axial profiles at the -12 degree position. The left center plot is the same data with 0th and 1st order terms removed. The center right and far right plots are similar data for the +13 degree azimuthal position.

Finally, difference plots for the -5V, 0V and +5V data are shown in Figure 14. Again, these images show that mounting deformations propagate through the mirror up to, but not far beyond neighboring mounting points, and that the local axial slope changes in a smooth fashion from the actuation point, dampening out by the next mounting point.

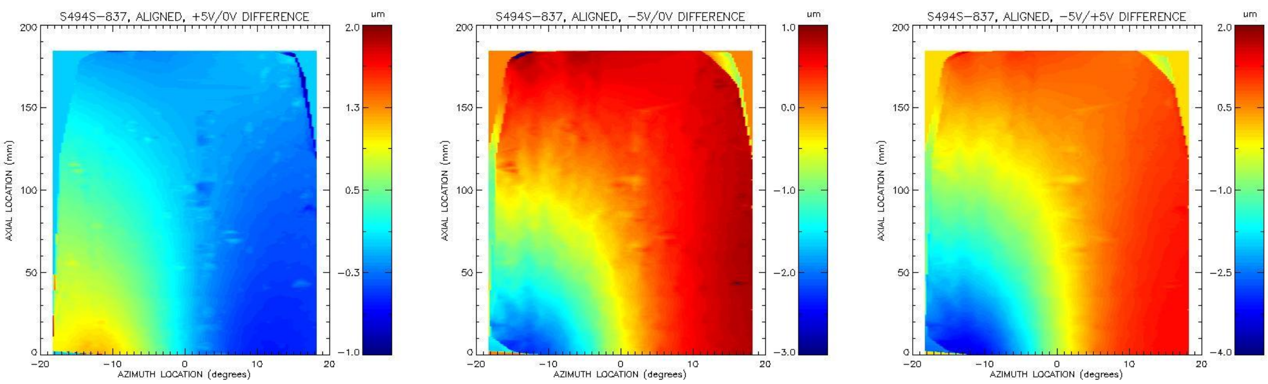

Figure 14. Difference maps for the -5V, 0V and +5V cases of the U2 actuator scan.

SUMMARY

The alignment process for the Constellation-X Spectroscopy X-ray Telescope has been significantly improved with the addition of an intermediate visible light collimated beam refinement step, and a new conical null lens. This new null lens allows us to image approximately 60% of the mirror segment through a high precision interferometer. The resulting figure maps provide the axial figure over a wide field of view while simultaneously being aligned with the Centroid Detector Assembly. The current expected imaging performance of the test mirror segment pair is 13.2 arcseconds HPD for 10 Å x-rays. We have also shown that the axial figure of mounted mirror segments is robust to mount and alignment induced deformations. Once the both mirror segments have been aligned and bonded into their respective housings, we will perform a full aperture x-ray imaging test at the Stray Light Facility at Marshall Space Flight Center.

[1] S. M. Owens, *et. al*, “Constellation-X SXT optical alignment Pathfinder 2: design, implementation, and alignment”, *Proc. SPIE* **5168**, 239 (2004).

[2] P. Glenn, “Centroid Detector Assembly for the AXAF-I Alignment Test System”, *Proc. SPIE* **2515**, 352 (1995).

[3] J. Hair, *et. al*, “Constellation-X Spectroscopy X-Ray Telescope Segmented Optic Assembly and Alignment Implementation”, *Proc SPIE* **4851**, 696 (2003).